

Prime Factorization Equation from a Tensor Network Perspective

Alejandro Mata Ali^{1*}, Jorge Martínez Martín^{1†}, Sergio Muñoz Subiñas^{1‡}, Miguel Franco Hernando^{1◦}, Javier Sedano^{1§} and Ángel Miguel García-Vico^{2¶}

¹ Instituto Tecnológico de Castilla y León, Burgos, Spain

² Andalusian Research Institute in Data Science and Computational Intelligence (DaSCI),
University of Jaén, 23071 Jaén, Spain

★ alejandro.mata@itcl.es, † jorge.martinez@itcl.es, ‡ sergio.muniz@itcl.es,
◦ miguel.franco@itcl.es, § javier.sedano@itcl.es, ¶ agvico@ujaen.es

Abstract

This paper presents an exact and explicit equation for prime factorization, along with an algorithm for its computation. The proposed method is based on the MeLoCoToN approach, which addresses combinatorial optimization problems through classical tensor networks. The presented tensor network performs the multiplication of every pair of possible input numbers and selects those whose product is the number to be factorized. Additionally, in order to make the algorithm more efficient, the number and dimension of the tensors and their contraction scheme are optimized. Finally, a series of tests on the algorithm are conducted, contracting the tensor network both exactly and approximately using tensor train compression, and evaluating its performance.

Copyright attribution to authors.

This work is a submission to SciPost Physics.

License information to appear upon publication.

Publication information to appear upon publication.

Received Date

Accepted Date

Published Date

Contents

1	Introduction	2
2	Background	3
3	Tensor Network for Factorization	3
3.1	Logical Circuit	4
3.1.1	Binary addition	4
3.1.2	Modular binary multiplication	6
3.1.3	Modular binary multiplication of two numbers	6
3.2	Tensor Network equation	7
3.3	Contraction scheme and computational complexity analysis	9
4	Performance evaluation and results	11
4.1	Exact case	11
4.2	Approximated case	12
5	Discussions	13

6	Conclusions	14
A	Tensor network definition	15
	References	17

1 Introduction

Prime factorization is the process of expressing a positive composite number N as the product of its prime factors; that is, finding all p_i that satisfy the equation $N = \prod_i p_i$. Despite its apparent simplicity, the problem is very difficult to solve; in fact, prime factorization is classified as NP. The problem has been studied for centuries due to its academic significance [1] and its foundational role in areas such as number theory or cryptography. This is of special interest for semiprime numbers, which are products of two prime numbers, so $N = pq$. This has led to the development of various prime factorization algorithms, including memcomputing techniques [2] and genetic algorithms [3]. However, a classical algorithm capable of factoring N in polynomial time has not yet been discovered. Consequently, the security of the widely used RSA [4] cryptographic algorithm depends on the difficulty of this problem, as deriving the private key from the public key requires the factorization of large numbers. This is an important topic in the cybersecurity field, and even more so in conflict contexts. The current record is the factorization of an RSA-240 number [5].

In this problem, quantum computing offers an advantage with Shor's algorithm for prime factorization [6–8], which has an exponential acceleration regarding the best known classical algorithms. In addition, there are other quantum algorithms, based on QUBO formulation [9] or variational circuits [10] that allow its resolution. Nevertheless, these algorithms are limited by the quality of current error-prone quantum hardware, which is why several alternative quantum-inspired technologies have been developed. One of the most interesting approaches is the use of tensor networks [11], consisting of the graphical representation of a tensor contraction equation. Unlike quantum computing algorithms, the tensor networks are computed in classical resources because it is a classical computation approach. This technology allows for efficient classical simulation of some low-entangled quantum systems by transforming them into tensor representations. An example is the Tensor Train (TT) representation [12], which consists of a linear chain of tensors connected to each other by their bond indices. These representations are useful for computing tensor network contractions, since they allow approximating the state at each step without requiring excessive scaling. This approach has been explored to break up to RSA-100 [13]. Another possible approach is the MeLoCoToN formalism [14] which allows obtaining the exact and explicit equation that solves inversion and optimization problems by using classical logical circuits and tensor networks. This approach has been applied to several optimization and constraint satisfaction problems, and as far as is known, never to the factorization case. A similar approach is presented in [15] for creating tensor networks that implement exactly arbitrary discrete linear constraints, more focused on tensor trains.

The main contributions of this work are as follows:

- An exact and explicit equation that solves the factorization problem for any given semiprime number, applicable to other types of numbers.
- An optimization of this equation to reduce computational resources, particularly in the

case of RSA.

- Two tensor network-based algorithms to compute the prime factorization result and an analysis of their computational complexity.
- An study of the computability of the correct result with compressions of tensor trains.

This work will be structured as follows. First, Sec. 2 introduces a brief background on the semiprime factorization algorithms. Secondly, Sec. 3 introduces the tensor network equation and algorithm. Then, Sec. 4 presents the experiments performed and their results. Finally, Sec. 5 discusses the results.

2 Background

In the field of semiprime factorization, there exist several algorithms and studies in the literature, due to their relevance. This section provides a brief background of the available algorithms, focusing on the most relevant ones. Obviously, this work will focus on odd numbers, because even numbers are trivially factorizable in 2 and $N/2$.

The first method is the Fermat factorization method, which consists of looking for a value a , which satisfies

$$N = a^2 - b^2 = (a + b)(a - b). \quad (1)$$

In this way, if $N = pq$, then

$$N = \left(\frac{p+q}{2}\right)^2 - \left(\frac{p-q}{2}\right)^2. \quad (2)$$

The algorithm starts from an initial value $a = \lceil \sqrt{N} \rceil$, and then calculates $b_2 = a^2 - N$. This process of increasing a by one unit is repeated until b_2 is a square. If N is a prime, it requires $O(N)$ steps, but if both numbers are similar, near \sqrt{N} , it is a fast algorithm to reach factorization. If it is combined with the trial division [16], its complexity is reduced to $O(N^{1/3})$ steps, which remains exponential with respect to the number of bits of N .

The second algorithm is Dixon's factorization method [17]. It is based on finding a congruence of squares modulo N such as Fermat's method. A bound B is imposed in order to define a base P of all primes equal to or lower than B . Then a set of values of z are selected, such that $z^2 \bmod N$ is B -smooth. With these values and linear algebra, it reaches the congruent pair of values a and b . Its complexity is $O(\exp(2\sqrt{2}\sqrt{\ln N \ln \ln N}))$.

The third algorithm is the Quadratic Sieve [18], the second-fastest method known in practice, being the fastest for integers under 100 decimal digits. It is a modification of Dixon's method, but it makes use of quadratic polynomials. Its complexity is conjectured to be $O(\exp((1 + O(1))\sqrt{\ln N \ln \ln N}))$.

The last classical method is the General Number Field Sieve [19], which is the most efficient classical algorithm known for this task for numbers larger than 10^{100} . Its complexity is $O(\exp(((64/9)^{1/3} + O(1))(\ln N)^{1/3}(\ln \ln N)^{2/3}))$.

In the quantum computing field, the most well-known algorithm is Shor's algorithm [6], which reduces the problem to looking for the period of a modular function. Its complexity is $O((\ln N)^2(\ln \ln N)(\ln \ln \ln N))$, polynomial in the number of bits of N [20].

3 Tensor Network for Factorization

This section introduces the tensor network equation and the algorithm to compute it. The MeLoCoToN formalism [14] is used to obtain the equation, and then design an optimized

algorithm to compute it. The MeLoCoToN formalism has three basic steps. First, it needs the creation of the classical logical circuit that computes the function to invert. In Sec. 3.1 is described the creation of the logical circuit of the function that performs the product of two prime odd numbers lower than N . The second step is to tensorize the logical circuit to obtain the tensor network that represents the logical space. The last step is to iterate on this tensor network, contracting it with other tensors to determine the correct value of each variable and getting the explicit equation. The last two steps are performed in Sec. 3.2, optimizing the size of the tensors involved. Finally, to obtain the solution values, it is necessary to contract these tensor networks, which requires a contraction scheme. In Sec. 3.3 two contraction schemes are provided, and an analysis of their computational complexity.

3.1 Logical Circuit

This subsection introduces the classical logical circuit that serves as the foundation for the tensor network. This logical circuit takes p and q , and returns $N = pq$. Instead of computing the usual product of two numbers, due to the target problem, it performs a capped binary multiplication between p and q , ensuring that the resulting product does not exceed the length of n , where n is the number of bits of N . This multiplication of two binary numbers p (multiplier) and q (multiplicand) is achieved by conditionally shifting and adding the multiplicand based on the bits of the multiplier.

To provide a clear understanding of the logical circuit, it is convenient to begin explaining the logic behind an adder circuit of two numbers in Sec. 3.1.1 and a modular binary multiplier of two numbers in Sec. 3.1.2. These are known operations in binary computing, but the former will be adapted to this problem. In these cases, the functions $f_q(p) = p + q$ and $g_q(p) = pq$ are computed, respectively. These functions receive only one of the numbers and then operate it with the other number, which is a parameter of the function. To create functions of two numbers, $f(p, q) = p + q$ and $g(p, q) = pq$, these types of circuits need to be generalized, as in Sec. 3.1.3.

3.1.1 Binary addition

To illustrate the binary adder to add an input p and a fixed q , consider a specific example where $p = p_2p_1p_0 = 111$ and $q = q_2q_1q_0 = 110$, shown in Fig. 1. Starting with the least significant bit, a bitwise addition is performed, resulting in the carry

$$c_0 = \left\lfloor \frac{p_0 + q_0}{2} \right\rfloor = 0$$

and the sum

$$N_0 = p_0 \oplus q_0 = 1$$

shown in Fig. 1 a. The next operator receives c_0 , p_1 and q_1 and computes

$$c_1 = \left\lfloor \frac{c_0 + p_1 + q_1}{2} \right\rfloor = 1$$

and

$$N_1 = c_0 \oplus p_1 \oplus q_1 = 0,$$

as shown in Fig. 1 b. The last operator receives c_1 , p_2 and q_2 and computes

$$c_2 = \left\lfloor \frac{c_1 + p_2 + q_2}{2} \right\rfloor = 1 = N_3$$

and

$$N_2 = c_1 \oplus p_2 \oplus q_2 = 1,$$

shown in Fig. 1 c. If final value c_2 is neglected, it performs the modular binary addition $(p + q) \bmod 2^n$.

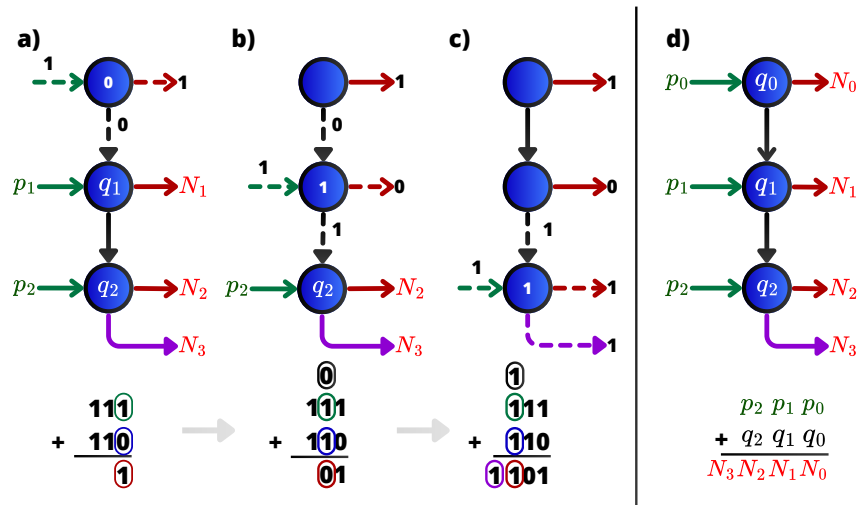


Figure 1: Logical circuit of the binary addition between two numbers. a), b) and c) represent each step of a binary addition between the numbers $p = 111$ and $q = 110$. d) Abstraction of the logical circuit of a binary addition of two numbers with 3 bits at most.

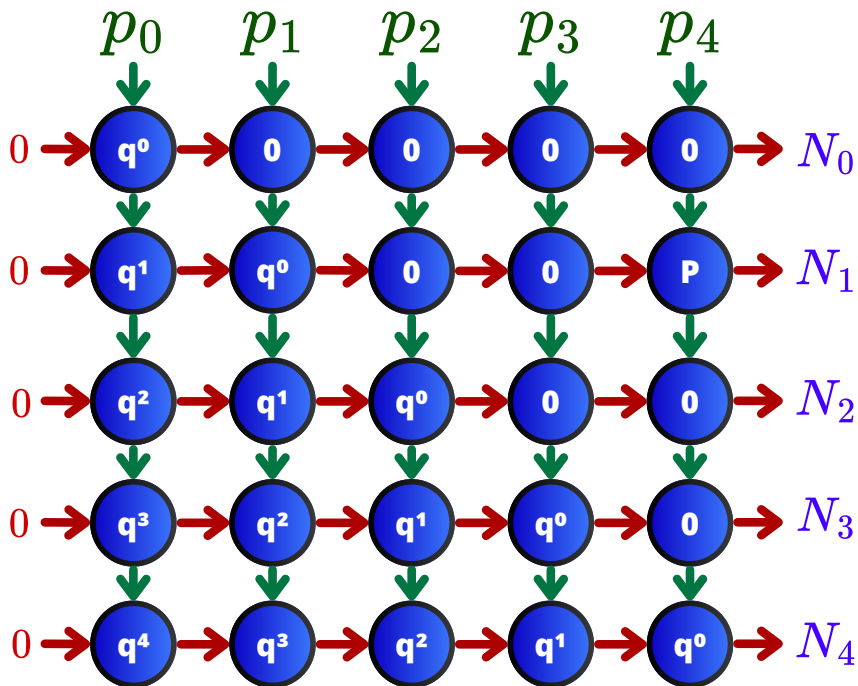


Figure 2: Logical circuit of the binary multiplication between two numbers p and q .

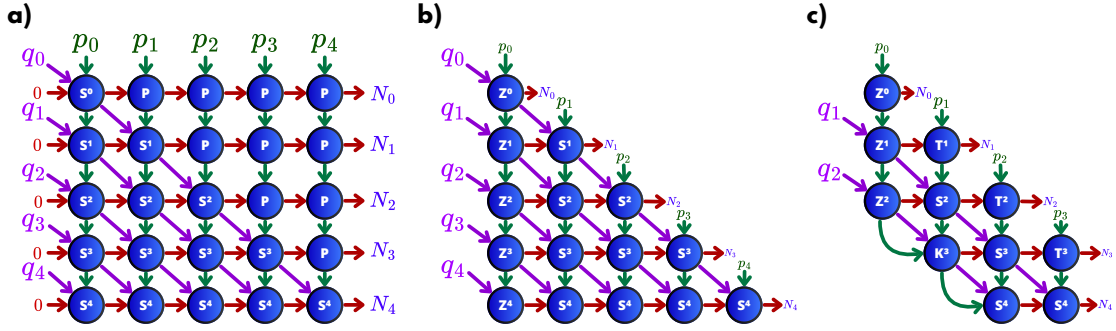


Figure 3: a) Logical circuit that performs the multiplication in binary terms of two numbers p and q of at most n bits, returning $N = pq$ of at most n bits. b) Logic circuit that performs the same calculation, eliminating the unnecessary P operators and $b_0 = 0$ input. c) Logic circuit in which the number q has up to $\lceil n/2 \rceil$ bits and the number p has up to $n - 1$ bits.

3.1.2 Modular binary multiplication

The logical circuit presented in Fig. 2 represents the modular binary multiplication of an input p and a fixed q based on Eq. 3. This logical circuit can be interpreted as a series of controlled additions. Taking into account the following property [7]

$$(qp) \bmod 2^n = (\dots((2^0 qp_0) \bmod 2^n + 2^1 qp_1) \bmod 2^n + \dots + 2^{n-1} qp_{n-1}) \bmod 2^n, \quad (3)$$

a modular multiplication can be performed by an iterative modular summation. Starting from zero, a concatenated set of modular additions of Fig. 1 are performed, each one adding $(2^k q) \bmod 2^n$ only if $p_k = 1$. To simplify the following computations, it must be considered that $(2^k q) \bmod 2^n$ is the same binary string as q , but neglect the k most significant bits and concatenate k zeros to its end. An example is that $(2 \times 5) \bmod 2^3 = 2$ is in binary $(2 \times 101) \bmod 2^3 = 010$. Then, the same addition layer can be used repeatedly, removing the operators of the neglected bits.

3.1.3 Modular binary multiplication of two numbers

In the previous section, it has been shown the logical circuit that computes $(qp) \bmod 2^n$ for an input p and a fixed q . However, some modifications are necessary to achieve the goal of designing a circuit capable of taking as input both p and q . Fig. 3 illustrates the generalization so that each layer k receives as horizontal input b_k (Eq. 4) and vertical input p_k .

$$b_{k+1} = b_k + 2^k qp_k = \sum_{j=0}^k 2^j qp_j, \quad b_0 = 0. \quad (4)$$

To ensure that the application of each q is consistent throughout all layers, it is sent as a diagonal signal, since the binary of $2x$ is the same number x shifted a bit. Taking into account that the target is a known value of N , to ensure that the output remains within the bit length of N , the final row imposes an overflow constraint by transmitting a zero signal in cases where the result exceeds the allowed bit length. In this way, it only returns the value if it is below 2^n .

As q is shifted one bit per layer, the first k operators of the k -th layer are operators that pass the control value p_k and the corresponding bit of b without modifying it. For this reason, these operators do not add any information and can be removed, leaving only the operators of the lower triangle (Fig. 3 b). Moreover, since the initial value b_0 is always 0, the first column

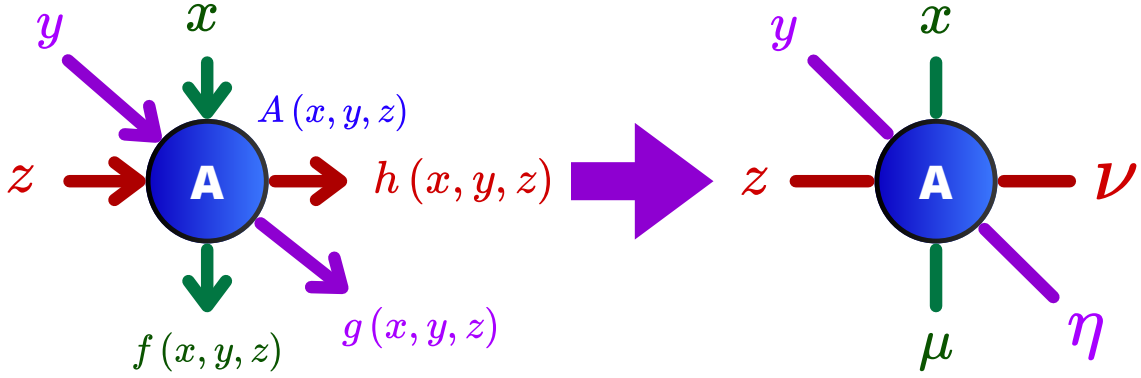


Figure 4: Tensorization of a six indexes operator with 3 inputs and 3 outputs that has an internal transformation $A_{x,y,z,\mu,\nu,\eta} = A(x,y,z) \delta_{\mu,f(x,y,z)} \delta_{\eta,g(x,y,z)} \delta_{\nu,h(x,y,z)}$. This means the resulting tensor has only non-zero elements $A_{x,y,z,\mu,\nu,\eta} = A(x,y,z)$ when $\mu = f(x,y,z)$, $\eta = g(x,y,z)$ and $\nu = h(x,y,z)$.

of operators can be directly applied to sum on the value 0, so that they do not receive an input b .

Without loss of generality, the asymmetric condition $q < p$ can be imposed, so $q < \sqrt{N}$, which limits the bit length of q to at most $\lceil n/2 \rceil$. In this way, half of the lower diagonals are removable since they only add up 0, which implies eliminating their associated operators as well. This means that for the operators of the following layers that start their bit, the input they receive from b will be the carry of the operator of the previous bit in the previous layer. Next, because the objective N is a semiprime, both p and q must be at most $\lfloor N/2 \rfloor$. Consequently, the most significant bit of p can be set to 0, eliminating its associated operator. Finally, since both numbers p and q are odd in this problem, the least significant bit of both has to be 1. This implies in the case of q that its first diagonal can be omitted, since it always passes 1. The resulting logic circuit is shown in Fig. 3 c.

3.2 Tensor Network equation

The next step is to tensorize the logical circuit, as explained in [14]. This process involves transforming the operators into their tensor representations by replacing each operator with a tensor which has as many indices as the total number of inputs and outputs of the operator. The transformation for a generic tensor is shown in Fig. 4 and the mathematical representations are defined in Appendix A.

Tensorization considers at the same time all possible q , allowing the algorithm to determine the bit values of p . In this formulation, the tensor network obtained after tensorizing the circuit represents the tensor T , where the non-zero elements satisfy $T_{x_0,x_1,x_2,\dots,y_0,y_1,y_2,\dots} = 1$ only if $y = qx$ for some q . This is a similar construction as the presented in [21]. This implies that this tensor network represents the function $f(x) = qx$ for all possible q at the same time. The main formalization and demonstration of this tensorization consequence is thoroughly studied in [14, 22].

To extract the correct value of p , the condition is imposed that the output y must be equal to N . This is achieved by projecting the tensor onto the subspace where the last indices satisfy $y = N$. This is equivalent to performing the contraction operation

$$T'_{x_0,x_1,x_2,\dots} = \sum_y T_{x_0,x_1,x_2,\dots,y_0,y_1,y_2,\dots} \delta_{y_0}^{N_0} \delta_{y_1}^{N_1} \delta_{y_2}^{N_2} \dots, \quad (5)$$

where δ^b is a vector of all zero elements except one equal to 1 at position b . To do this, a δ^{N_k} vector is connected to each k -th output index. This causes the only non-zero element of the

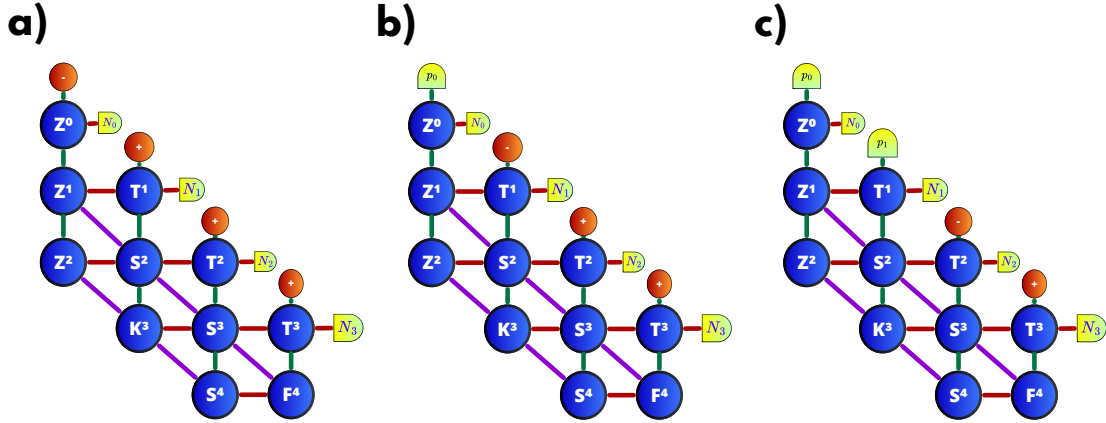


Figure 5: Tensor network of the prime factorization for five bits number N which determines the a) first bit of p , b) second bit of p , c) third bit of p .

T' tensor to be $T'_{x_0, x_1, x_2, \dots} = 1$, for all the inputs x that generate the output N through $N = qx$. That is,

$$T'_{x_0, x_1, x_2, \dots} = \delta_{x_0}^{p_0} \delta_{x_1}^{p_1} \delta_{x_2}^{p_2} \dots \quad (6)$$

From the tensor network, obtaining p can be achieved using the iterative Half Partial Trace [14]. In summary, this method extracts the position of the non-zero element through an iterative process, determining one bit at a time. If there is only one non-zero element, in case of summing over all the indices except the z index, the resulting vector will have its non-zero element at the value of the index that matches the corresponding value of that index in the original tensor that has the non-zero element. That is, if the tensor is $T'_{x_0, x_1, x_2, \dots}$, and a sum is performed on all the indexes but x_0 , the new vector V has elements

$$\begin{aligned} V_{x_0} &= \sum_{x_1, x_2, \dots} \left(T'_{x_0, x_1, x_2, \dots} \prod_{i=1} \mathbf{1}_{x_i} \right) = \\ &= \delta_{x_0}^{p_0} \prod_{i=1} \left(\sum_{x_i} \delta_{x_i}^{p_i} \mathbf{1}_{x_i} \right) = \delta_{x_0}^{p_0} \prod_{i=1} 1 = \delta_{x_0}^{p_0}, \end{aligned} \quad (7)$$

being $\mathbf{1}$ ones vectors. This is performed by connecting to each input index, but the one of the variable to be determined, a ones vector.

Thus, the correct value of each variable corresponds to the position of the 1 in the resulting vector. To avoid working directly with a vector and obtain a closed equation, the vector has to be transformed into a scalar. To do this, the tensor network is multiplied by the vector $(-1, 1)$, so if the original vector is $(1, 0)$, the value of the resulting scalar is -1 , if it is $(0, 1)$ the result is 1 , and if it is $(1, 1)$ because there are two possibilities, it is 0 . Using this approach, $p_k = H(\Omega_k)$ is defined, where H is the Heaviside step function and Ω_k is the value of the contraction of the tensor network obtained at the k -th iteration. At each iteration, since the values of the previously determined bits of p are known, these values are enforced as inputs by replacing the generic $(1, 1)$ vectors with the $\delta_{x_j}^{p_j}$ -tensors. In this case, because there is only one solution, the problem does not have degeneration, implying that every variable result is independent from the other. Then this imposition is not necessary in the exact case, but it is used in the approximation case.

The defined tensor network is illustrated in Fig. 5, where in order to determine each variable, the results obtained previously are imposed. It can be solved from the least significant bit to the most significant bit, as shown in Fig. 5, or from the most significant to the least. This

will depend on the contraction scheme and the compression process used. However, to obtain the exact solution, this is not required.

Theorem 1 (Semiprime factorization equation) *Given a known odd semiprime integer positive number N , which satisfies $N = pq$ for some different p and q positive prime numbers greater than 1, then the value of p is determined by the exact and explicit equation*

$$P = p_{n-1}p_{n-2} \cdots p_1p_0, \quad p_k = H(\Omega_k), \quad (8)$$

being $H(\cdot)$ the Heaviside step function and Ω_k the k -th tensor network defined by the MeLoCoToN construction.

It is interesting to note that certain constraints can be removed from the equation by adding more complexity to the tensor network. The odd condition can be removed by introducing the first diagonal, allowing the value 0 for the less significant bit of q . The inequality can be considered $q \leq p$ allowing the $q = \sqrt{N}$ and $q = 1$ cases simply by not removing the last tensor layer. More general can be factorized by using the enforcement of previous results, and obtaining in each iteration group one of the numbers of the factorization, repeating the process more times.

3.3 Contraction scheme and computational complexity analysis

With the tensor network equation defined, the results of the equation can be computed with a contraction scheme, the order chosen for the contractions of the pairs of tensors of the network. In this section, the computational complexity of computing the matrix-matrix multiplication

$$C = \sum_{i,j,k}^{I,J,K} A_{ij} B_{jk} \hat{e}_i \hat{e}_k \quad (9)$$

is assumed to be $O(IJK)$.

The tensor network contraction scheme can be performed mainly in two ways: from bottom to top and from left to right. In the bottom-up case, each tensor of the last row is contracted from right to left, until the whole row is contracted. Since in the last step, a tensor of $n - 1$ indices of dimensions

$$\underbrace{(2, \dots, 2)}_{n/2-1}, \underbrace{(3, \dots, 3)}_{n/2-1}, 4)$$

is contracted with one of three indices of dimensions $(4, 3, 2)$, through its dimension 4 index, the computational complexity of contracting this row is $O(4(2 \cdot 3)^{n/2}) = O(6^{n/2})$. After that, this tensor is contracted with each tensor of the next row, from right to left, until the entire row is fully contracted. In this case, each contraction has a cost of $O(6^{n/2})$, and for the whole row, $O(n6^{n/2})$. Applying this contraction process to all rows results in an overall complexity of $O(n^2 6^{n/2})$. Moreover, since this procedure must be repeated $O(n)$ times in the iterative process to determine each bit of p , the total cost is $O(n^3 6^{n/2})$. In terms of N , the computational complexity is $O((\log_2 N)^3 6^{\log_2 \sqrt{N}})$ or $O((\ln N)^3 \exp((\log_2 \sqrt{6}) \ln N))$. This complexity is worse than the brute force complexity. The contraction scheme is shown in Fig. 6.

In the left-to-right case, it is contracted following the same style. First, the initial column is contracting from top to bottom and then with the following columns from top to bottom. Since the tensors have dimension $O(4^{n/2})$, the cost of contracting each column is $O(n4^{n/2})$. Repeating this for n columns results in a complexity of $O(n^2 4^{n/2})$ per iteration, which to obtain the n bits of p results in a total cost of $O(n^3 4^{n/2})$. In terms of N , the computational complexity is $O((\log_2 N)^3 4^{\log_2 \sqrt{N}})$ or $O((\ln N)^3 N)$. This complexity is also worse than the brute force complexity. The contraction scheme is shown in Fig. 7.

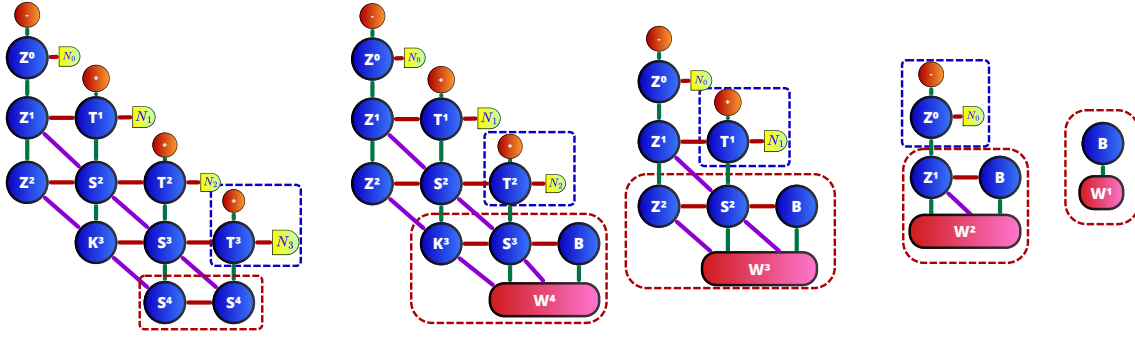


Figure 6: Exact contraction scheme from bottom-up. Last row is contracted, and the resulting tensor is contracted with the the row above it from right to left.

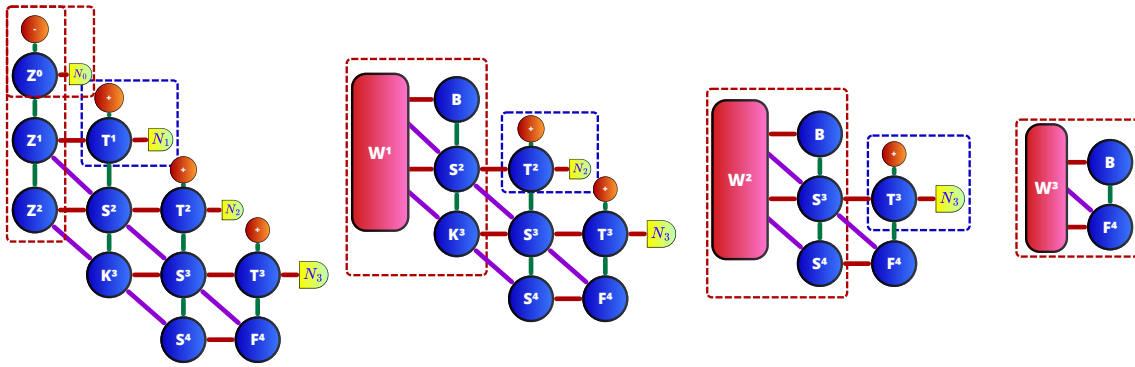


Figure 7: Exact contraction scheme from left-right. First column is contracted, and the resulting tensor is contracted with the the row above it from top to bottom.

It is important to note that both computational complexities are calculated without taking into account the high sparsity of the contracted tensors, so it could be improved. The tensor creation complexity is negligible because each type of tensor is created only once, and then repeated in the contraction. In case all tensors are created in the first step, it would require $O(n^2)$ time, because the grid has that amount of tensors in the grid.

In both scenarios, the time complexity and the required memory scale exponentially in the number of bits of N . In an attempt to overcome this limitation, the possibility of computing this equation in an approximate way is evaluated. The complexity is due to the high size of the tensors in the intermediate computations. However, the initial tensor of the row or column has minimal entanglement, and the result must be a tensor product of vectors. Both the input of the problem N and the output p are products, so they can be represented by a matrix product state (MPS), or tensor train (TT) of bond dimension 1. This means that, by Rolle's theorem, the correlations grow up to some step of the contraction, and, after that, they decrease until the end of the process. If during the contraction, the intermediate tensor is represented as an approximated TT to compress it, the exponential scaling could be avoided. The compression process consists of taking a TT representing a tensor and computing another tensor train with lower bond dimension (i.e. fewer elements) that represents a tensor similar to the original one. Taking into account that the problem has several symmetries and internal rules, it seems natural that the intermediate tensors should be compressible.

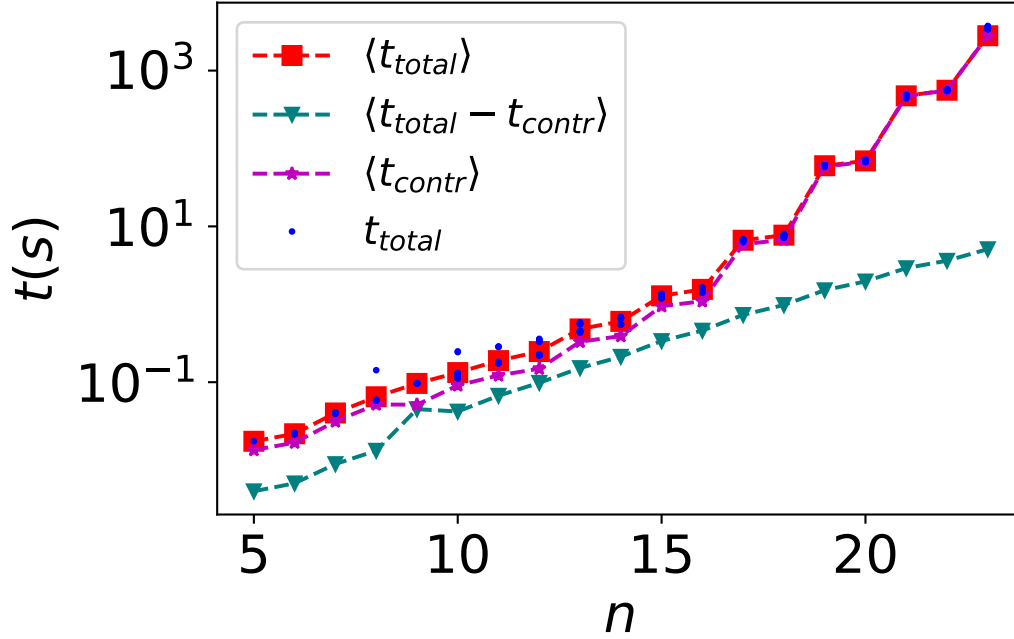


Figure 8: Execution time vs number n of bits of N . In blue points the time for each instance and in red squares the average total time. The purple star are the contraction time and the green triangles are the rest of time.

4 Performance evaluation and results

In this section, the correctness of the presented equation and the performance of its calculation are evaluated. The exact case is implemented by means of bottom-up contraction, to better evaluate the computational time scaling in Sec. 4.1. In Sec. 4.2, the approximated case is studied, and the minimum bond dimension needed to obtain the correct result is determined depending on the problem size. Finally, it is studied whether there is a dependence of the number of erroneous bits in the solution obtained on the ratio between the bond size used and that required in the failed cases.

For all these tests, ten numbers are used to factorize for each value of n (if available), so that the prime numbers used for the construction of N are not excessively different. This is to take the worst case, since if one is much smaller than another, the problem is simpler to solve. The runs have been performed on a regular laptop CPU Intel(R) Core(TM) i7-14700HX 2.10 GHz, with 32GB RAM and 20 cores, using the Python Tensorkrowch [23] library.

4.1 Exact case

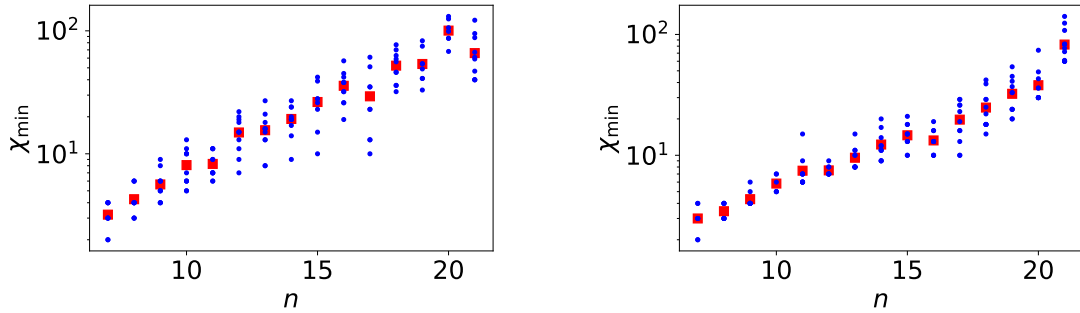
The first step is to compute the result of the equation with the presented contraction schemes. The contraction is performed using a bottom-up scheme. In addition, the time t_{total} is evaluated, defined as the time needed to obtain the solution from the moment the number N is introduced into the function to the moment the result is retrieved and the contraction time t_{contr} . No early stopping or bit prefixing at 0 is implemented to avoid biasing the evaluation.

As expected, in every attempt, the equation provides the correct number p . Fig. 8 shows the total time of each execution, the average for each problem size, the average contraction

time, and the average of the time which is not due to the contraction. As previously predicted, execution time scales exponentially with the n number of bits of N , and its main contribution is the contraction time. However, the exponential scaling of the time not related to the contraction may indicate that the implementation of the creation of the tensors and the processing of the data could be improved. These implementation problems may explain the slightly ascending curvature of the contraction time. It is also shown that the times do not have a relevant dispersion, probably caused by its execution on a regular laptop.

4.2 Approximated case

Now, the focus is to compute it more efficiently using an approximate train tensor. Figs. 9 show the minimum bond dimension needed to obtain the correct solution for each instance, and the average for each value of n . Fig. 9a shows the bottom-up contraction, and Fig. 9b shows the left-right contraction.



(a) Minimal bond dimension χ_{\min} vs number n of bits of N for bottom-up scheme. In blue points the dimension for each instance and in red squares the average dimension.

(b) Minimal bond dimension χ_{\min} vs number n of bits of N for left-right scheme. In blue points the dimension for each instance and in red squares the average dimension.

Figure 9: Minimal bond dimension χ_{\min} vs number n of bits of N for different contraction schemes.

It can be observed that the minimum bond dimension grows exponentially with the number of bits of the number to factorize. This implies that the algorithm continues to scale exponentially with the size of the problem. However, the scaling is much smaller than in the exact case since it arrives at bond dimensions much smaller than what would be expected in the exact case. The minimum bond dimension in the exact uncompressed case is

$$r_{\max} = \sqrt{6^{n/2}}, \quad r_{\max} = \sqrt{4^{n/2}}, \quad (10)$$

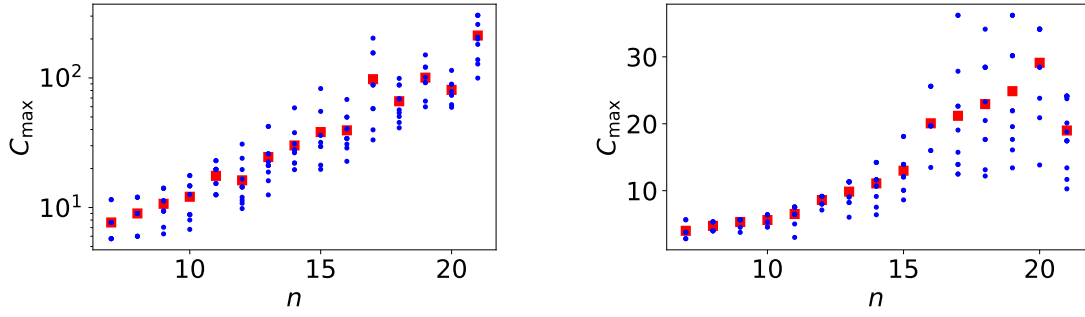
for the bottom-up scheme and the left-right scheme, respectively, so the compression factor is defined as

$$C_{\max} = \frac{r_{\max}}{\chi_{\min}}. \quad (11)$$

As can be seen in Figs. 10, the scaling of the compression factor is also exponential with respect to n . This indicates that there is not as much entanglement in the system as was initially considered and that there may be a more efficient tensor network to solve the problem.

An interesting point of study is to check if there is a dependence between the required bond dimension and the number of zeros in one of the prime factors. The proportion of zeros is defined as

$$n_0 = \frac{n(p, 0)}{n(p, 0) + n(p, 1)}, \quad (12)$$

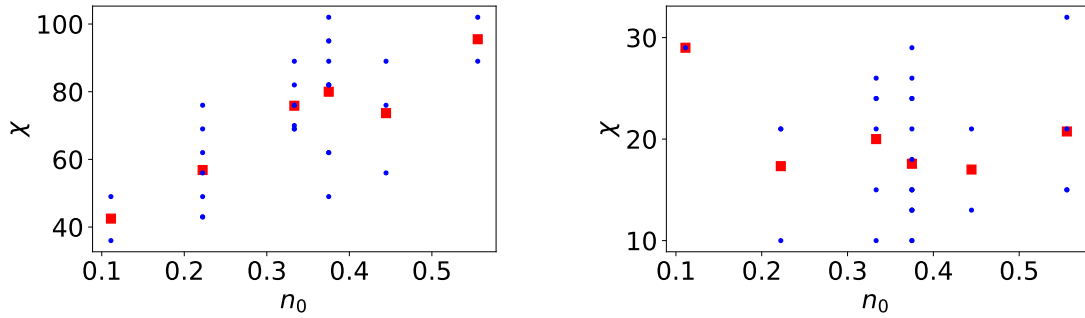


(a) Maximum possible compression vs number n of bits of N for bottom-up scheme.

(b) Maximum possible compression vs number n of bits of N for left-right scheme.

Figure 10: Maximum possible compression vs number n of bits of N for different contraction schemes.

being $n(x, y)$ the number of bits with value y in binary form of x . The results of Figs. 11 show a relation cannot be directly deduced in the left-right scheme, but it seems that there may be a dependency in the bottom-up. However, given the sample, no relation can be concluded.



(a) Minimal bond dimension vs n_0 for $n = 16$ with $p = 179$ for bottom-up scheme.

(b) Minimal bond dimension vs n_0 for $n = 16$ with $p = 179$ for left-right scheme.

Figure 11: Minimal bond dimension vs n_0 for different contraction schemes.

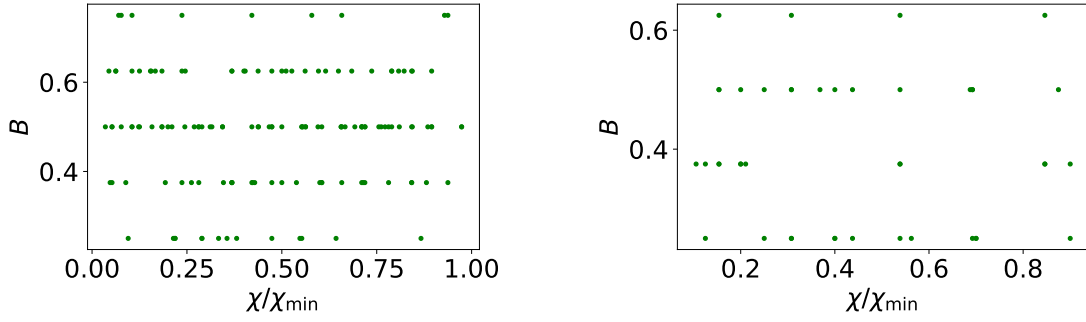
Finally, it is checked if there is a possibility that, although the bond dimension used is lower than the minimum necessary, the result obtained allows us to obtain part of the information of the correct solution. The bit-flip error is defined as

$$B = \sum_{i=0}^{n-1} \frac{(1 - x_i)p_i + x_i(1 - p_i)}{n}. \quad (13)$$

As can be seen in Figs. 12, there does not appear to be any relationship between the level of error and the increase in bond dimension.

5 Discussions

This work has presented an exact and explicit equation that allows factoring an odd semiprime number into its prime factors. However, its computation requires an exponential amount of time and memory, making its use worse than the brute force search for these factors. This



(a) Bit-flip rate B vs the proportion $\frac{\chi}{\chi_{\min}}$ for bottom-up scheme.

(b) Bit-flip rate B vs the proportion $\frac{\chi}{\chi_{\min}}$ for left-right scheme.

Figure 12: Bit-flip rate B vs the proportion $\frac{\chi}{\chi_{\min}}$ for different contraction schemes.

equation has been computed with classical computational resources and its correctness and exponential scaling have been verified. In the approximated computation, the tensor train compression has been studied to improve its performance, but the results remain exponential. Nevertheless, the results, with high compression, indicate to us that there could exist a more efficient tensor network equation, and its computation could be more efficient. This is consistent with the high sparsity of all the tensors, even the intermediate ones. The no relation between the number of zeroes and the minimal bond dimension is certainly unexpected, because more equal digits may require simpler rules to implement. In addition, the absence of a relation between the bit-flip error and the bond dimension below the minimum required dimension is an interesting result. This may indicate that the system must either have the necessary bond dimension or it does not allow any information to be extracted from the correct solution. Both results could be a consequence of the tensor train representation, because its natural expressibility remains in one-dimensional relations, and the bit information does not correspond to a one-dimensional phenomenon. This opens the possibility of studying other tensor network representations for the compressed contraction.

6 Conclusions

Even with these computational results, this work has provided the first exact and explicit equation for the computation of the solutions of the problem. Its computation with tensor network contraction schemes has been studied, but there could be other more efficient ways to compute it. For example, if there could be a physical system that could efficiently compute this equation, it could be used to factorize semiprime numbers. This opens a new future research line in analog computing. Another possible way is to use mathematical properties of the equation to simplify it. For example, the equation is the contraction of several Kronecker delta tensors, and they can be decomposed into the contraction of other tensors. In this way, it could be applied to avoid certain computations. This opens up new research lines in pure mathematics and computational mathematics. Another possible research line from this work is the study of other tensor representations for compressed contraction, making use of the sparsity to improve the complexity and obtain a new tensor network that is easier to contract. Finally, this work provides a new perspective of how to approach this problem, and similar ones, with a simple tensor network construction, being the starting point for applying it to several other fundamental mathematical and cybersecurity problems.

Data and code availability

All data and code required for this project can be accessed upon reasonable request by contacting the authors.

Acknowledgements

Funding information The research has been funded by the Ministry of Science and Innovation and CDTI under ECOSISTEMAS DE INNOVACIÓN project ECO-20241017 (EIFEDE) and ICECyL (Junta de Castilla y León) under project CCTT5/23/BU/0002 (QUANTUMCRIP). This project has been funded by the Spanish Ministry of Science, Innovation and Universities under the project PID2023-149511OB-I00, and under the programme for mobility stays at foreign higher education and research institutions "José Castillejo Junior" with code CAS23/00340.

A Tensor network definition

There are the following types of tensors that make up the tensor network, to factorize an N number of n bits, allowing p to have up to $n - 1$ bits and q to have up to $\lceil n/2 \rceil$ bits.

Initial layer The first column is composed of three types of tensors, the initial $Z_{2 \times 2 \times 2}^0$ that connects to bit p_0 and bit N_0 ,

$$\begin{aligned} v &= \mu = j, \\ Z_{j\mu v}^0 &= 1, \end{aligned} \tag{A.1}$$

the intermediate $Z_{2 \times 2 \times 2 \times 2}^k$ for the intermediate rows,

$$\begin{aligned} v &= j, \\ \mu &= jl, \\ Z_{jl\mu v}^k &= 1, \end{aligned} \tag{A.2}$$

and the last $Z_{2 \times 2 \times 4}^{\lceil n/2 \rceil}$ for the last row of the layer, carrying the most significant bit of q ,

$$\begin{aligned} \mu &= jl, \\ Z_{j\mu l}^{\lceil n/2 \rceil} &= 1. \end{aligned} \tag{A.3}$$

Presaturation layers The columns before saturation are composed of three types of tensors, the initial $T_{2 \times 2 \times 2 \times 3}^k$ that connects to bit p_k and bit N_k ,

$$\begin{aligned} \mu &= i \oplus j, \\ v &= j(i + 1), \\ T_{ij\mu v}^k &= 1, \end{aligned} \tag{A.4}$$

the intermediate $S_{2 \times 3 \times 2 \times 2 \times 3 \times 2}^k$, for the intermediate rows,

$$\begin{aligned} c &= \lceil j/2 \rceil, \quad y = j - c, \\ \mu &= i \oplus c(l \oplus y), \\ v &= c \left(1 + \left\lfloor \frac{i + l + y}{2} \right\rfloor \right), \\ \eta &= l, \\ S_{ijl\mu v\eta}^k &= 1, \end{aligned} \tag{A.5}$$

and the last $K_{3 \times 4 \times 2 \times 4}^k$, for the last row of the layer, carrying the most significant bit of q ,

$$\begin{aligned} c &= \lceil j/2 \rceil, \quad y = j - c, \\ y_i &= \lfloor l/2 \rfloor, \quad y_l = l \pmod{2}, \\ \mu &= y_i \oplus c(y_l \oplus y), \\ \eta &= 2 \left\lfloor \frac{y_i + c(y_l + y)}{2} \right\rfloor + y_l, \\ K_{j\eta\mu}^k &= 1. \end{aligned} \tag{A.6}$$

Saturation Layer The column of saturation is composed of three types of tensors, the initial $T_{2 \times 2 \times 2 \times 3}^k$ that connects to bit p_k and bit N_k as before, the intermediate $S_{2 \times 3 \times 2 \times 2 \times 3 \times 2}^k$, for the intermediate rows as before, and the last $S_{3 \times 4 \times 2 \times 4}^{n-1}$, for the last row of the layer, carrying the most significant bit of q and informing the following layers if its bit has been in 1.

Their non-zero elements are

$$\begin{aligned} c &= \lceil j/2 \rceil, \quad y = j - c, \\ y_i &= \lfloor l/2 \rfloor, \quad y_l = l \pmod{2} \\ \left\lfloor \frac{y_i + c(y_l + y)}{2} \right\rfloor &= 0, \\ \mu &= 2y_l + y_i \oplus c(y_l \oplus y), \\ S_{j\eta\mu}^{n-1} &= 1. \end{aligned} \tag{A.7}$$

Post-saturation layer The columns after saturation are composed of three types of tensors, the initial $T_{2 \times 2 \times 2 \times 3}^k$ that connects to bit p_k and bit N_k as before, the intermediate $S_{2 \times 3 \times 2 \times 2 \times 3 \times 2}^k$, for the intermediate rows as before, and the last $R_{4 \times 3 \times 2 \times 4}^{n-1}$, for the last row of the layer, carrying the most significant available bit of q and informing the following layers if its bit has been in 1.

Its non-zero elements are

$$\begin{aligned} c &= \lceil j/2 \rceil, \quad y = j - c, \\ y_s &= \lfloor i/2 \rfloor, \quad y_i = i \pmod{2}, \\ c y_s(l + y) &= 0, \left\lfloor \frac{y_i + c(l + y)}{2} \right\rfloor = 0, \\ \mu &= 2l + y_i \oplus c(l \oplus y), \\ R_{ijl\mu}^{n-1} &= 1. \end{aligned} \tag{A.8}$$

Final layer The final column after is composed of two types of tensors, the initial $T_{2 \times 2 \times 2 \times 3}^{n-2}$ that connects to bit p_{n-2} and bit N_{n-2} as before, and the last tensor $F_{4 \times 3 \times 2}^{n-1}$, for the last row of the layer, which imposes the final bit of N to be 1.

Its non-zero elements are

$$\begin{aligned}
 c &= \lceil j/2 \rceil, \quad y = j - c, \\
 y_s &= \lfloor i/2 \rfloor, \quad y_i = i \pmod{2}, \\
 \text{if } y_s &= 1 \Rightarrow c(l + y) = 0, \\
 \left\lceil \frac{y_i + c(l + y)}{2} \right\rceil &= 0, \\
 y_i \oplus c(l \oplus y) &= 1, \\
 F_{ijl}^{n-1} &= 1.
 \end{aligned} \tag{A.9}$$

References

- [1] L. Montgomery, *A survey of modern integer factorization algorithms*, CWI quarterly **7**, 337 (1994).
- [2] T. Sharp, R. Khare, E. Pederson and F. L. Traversa, *Scaling up prime factorization with self-organizing gates: A memcomputing approach*, doi:[10.48550/arXiv.2309.08198](https://doi.org/10.48550/arXiv.2309.08198) (2023), [2309.08198](https://doi.org/10.48550/arXiv.2309.08198).
- [3] M. A. Mobin and M. Kamrujjaman, *Cryptanalysis of rsa cryptosystem: Prime factorization using genetic algorithm*, doi:[10.48550/arXiv.2407.05944](https://doi.org/10.48550/arXiv.2407.05944) (2024), [2407.05944](https://doi.org/10.48550/arXiv.2407.05944).
- [4] R. L. Rivest, A. Shamir and L. Adleman, *A method for obtaining digital signatures and public-key cryptosystems*, Commun. ACM **21**(2), 120–126 (1978), doi:[10.1145/359340.359342](https://doi.org/10.1145/359340.359342).
- [5] F. Boudot, P. Gaudry, A. Guillevis, N. Heninger, E. Thomé and P. Zimmermann, *Comparing the difficulty of factorization and discrete logarithm: A 240-digit experiment*, In D. Micciancio and T. Ristenpart, eds., *Advances in Cryptology – CRYPTO 2020*, pp. 62–91. Springer International Publishing, Cham, ISBN 978-3-030-56880-1, doi:[10.1007/978-3-030-56880-1_3](https://doi.org/10.1007/978-3-030-56880-1_3) (2020).
- [6] P. Shor, *Algorithms for quantum computation: discrete logarithms and factoring*, In *Proceedings 35th Annual Symposium on Foundations of Computer Science*, pp. 124–134, doi:[10.1109/SFCS.1994.365700](https://doi.org/10.1109/SFCS.1994.365700) (1994).
- [7] S. Beauregard, *Circuit for shor’s algorithm using $2n+3$ qubits*, Quantum Info. Comput. **3**(2), 175–185 (2003), doi:[10.26421/QIC3.2-8](https://doi.org/10.26421/QIC3.2-8).
- [8] T. Häner, M. Roetteler and K. M. Svore, *Factoring using $2n + 2$ qubits with toffoli based modular multiplication*, Quantum Info. Comput. **17**(7–8), 673–684 (2017), doi:[10.26421/QIC17.7-8](https://doi.org/10.26421/QIC17.7-8).
- [9] K. Jun and H. Lee, *Hubo and qubo models for prime factorization*, Scientific Reports **13**(1) (2023), doi:[10.1038/s41598-023-36813-x](https://doi.org/10.1038/s41598-023-36813-x).
- [10] M. Sobhani, Y. Chai, T. Hartung and K. Jansen, *Variational quantum eigensolver approach to prime factorization on ibm’s noisy intermediate scale quantum computer*, Phys. Rev. A **111**, 042413 (2025), doi:[10.1103/PhysRevA.111.042413](https://doi.org/10.1103/PhysRevA.111.042413).
- [11] J. Biamonte and V. Bergholm, *Tensor networks in a nutshell*, doi:[10.48550/arXiv.1708.00006](https://doi.org/10.48550/arXiv.1708.00006) (2017), [1708.00006](https://doi.org/10.48550/arXiv.1708.00006).

- [12] I. V. Oseledets, *Tensor-train decomposition*, SIAM Journal on Scientific Computing **33**(5), 2295 (2011), doi:[10.1137/090752286](https://doi.org/10.1137/090752286), <https://doi.org/10.1137/090752286>.
- [13] M. Tesoro, I. Siloi, D. Jaschke, G. Magnifico and S. Montangero, *Quantum inspired factorization up to 100-bit rsa number in polynomial time*, doi:[10.48550/arXiv.2410.16355](https://doi.org/10.48550/arXiv.2410.16355) (2024), [2410.16355](https://doi.org/10.48550/arXiv.2410.16355).
- [14] A. M. Ali, *Explicit solution equation for every combinatorial problem via tensor networks: Melocoton*, doi:[10.48550/arXiv.2502.05981](https://doi.org/10.48550/arXiv.2502.05981) (2025), [2502.05981](https://doi.org/10.48550/arXiv.2502.05981).
- [15] J. Lopez-Piqueres and J. Chen, *Cons-training tensor networks: Embedding and optimization over discrete linear constraints*, SciPost Phys. **18**, 192 (2025), doi:[10.21468/SciPostPhys.18.6.192](https://doi.org/10.21468/SciPostPhys.18.6.192).
- [16] R. S. Lehman, *Factoring large integers*, Mathematics of Computation **28**(126), 637 (1974), doi:[10.2307/2005940](https://doi.org/10.2307/2005940).
- [17] J. D. Dixon, *Asymptotically fast factorization of integers*, Mathematics of Computation **36**, 255 (1981).
- [18] C. Pomerance, *The quadratic sieve factoring algorithm*, In T. Beth, N. Cot and I. Ingemarsson, eds., *Advances in Cryptology*, pp. 169–182. Springer Berlin Heidelberg, Berlin, Heidelberg, ISBN 978-3-540-39757-1, doi:[10.1007/3-540-39757-4_17](https://doi.org/10.1007/3-540-39757-4_17) (1985).
- [19] A. Lenstra, H. Lenstra, M. Manasse and J. Pollard, *The number field sieve*, In *Proceedings of the 22nd Annual ACM Symposium on Theory of Computing*, pp. 564–572, doi:[10.1145/100216.100295](https://doi.org/10.1145/100216.100295) (1990).
- [20] P. W. Shor, *Polynomial-time algorithms for prime factorization and discrete logarithms on a quantum computer*, SIAM Journal on Computing **26**(5), 1484–1509 (1997), doi:[10.1137/s0097539795293172](https://doi.org/10.1137/s0097539795293172).
- [21] S. Kourtis, C. Chamon, E. R. Mucciolo and A. E. Ruckenstein, *Fast counting with tensor networks*, SciPost Phys. **7**, 060 (2019), doi:[10.21468/SciPostPhys.7.5.060](https://doi.org/10.21468/SciPostPhys.7.5.060).
- [22] A. M. Ali, *Ftnilo: Explicit multivariate function inversion, optimization and counting, cryptography weakness and riemann hypothesis solution equation with tensor networks*, doi:[10.48550/arXiv.2505.05493](https://doi.org/10.48550/arXiv.2505.05493) (2025), [2505.05493](https://doi.org/10.48550/arXiv.2505.05493).
- [23] J. R. Pareja Monturiol, D. Pérez-García and A. Pozas-Kerstjens, *TensorKrowch: Smooth integration of tensor networks in machine learning*, Quantum **8**, 1364 (2024), doi:[10.22331/q-2024-06-11-1364](https://doi.org/10.22331/q-2024-06-11-1364), [2306.08595](https://doi.org/10.22331/q-2024-06-11-1364).